3D Scanning and 3D Printing as Innovative Technologies for Fabricating Personalized Topical Drug Delivery Systems

Alvaro Goyanes[1], Usanee Det-Amornrat[1], Jie Wang[1], Abdul W. Basit[1,2,*], Simon Gaisford[1,2,*]

[1]UCL School of Pharmacy, University College London, 29-39 Brunswick Square, London, WC1N 1AX, UK

[2]FabRx Ltd., 3 Romney Road, Ashford, Kent, TN24 0RW, UK

Corresponding authors:
a.basit@ucl.ac.uk
s.gaisford@ucl.ac.uk
Tel: 020 7753 5865

Key words

Three dimensional printing; fused deposition modelling; stereolithography; salicylic acid; hot melt extrusion

Abstract

Acne is a multifactorial inflammatory skin disease with high prevalence. In this work, the potential of 3D printing to produce flexible personalized-shape anti-acne drug loaded devices was demonstrated by two different 3D printing technologies: Fused Deposition Modeling (FDM) and stereolithography (SLA). 3D scanning technology was used to obtain a 3D model of a nose adapted to the morphology of an individual. Salicylic acid used in the treatment of acne was selected as a model drug (theoretical drug loading 2%w/w).

In FDM 3DP, commercially produced Flex EcoPLA^{TM} (FPLA) and polycaprolactone (PCL) filaments were loaded with salicylic acid by hot melt extrusion (HME). Drug loading in the FPLA-salicylic acid and PCL-salicylic acid filaments after HME was 0.6% w/w and 1.3% w/w respectively (showing significant thermal degradation of drug was observed during 3D printing). Diffusion testing in Franz cells using a synthetic membrane revealed that the drug loaded printed samples released less than 187 μg/cm^2 of their drug content within 3 h. FPLA-salicylic acid filament was successfully printed as a nose-shape mask by FDM 3DP, but the PCL-salicylic acid filament was not.

In the SLA printing process, the drug was dissolved in different mixtures of poly(ethylene glycol) diacrylate (PEGDA) and poly(ethylene glycol) (PEG) that were solidified by the action of a laser beam. SLA printing led to 3D printed devices (nose-shape) with higher resolution and higher drug loading (1.9% w/w) than FDM, with no drug degradation. The results of drug diffusion tests revealed that drug release was faster than with the FDM devices, 229 and 291 μg/cm^2 within 3 h for the two formulations evaluated.

In this study, SLA printing was a more appropriate 3D printing technology to manufacture anti-acne devices with salicylic acid. The combination of 3D scanning and 3D printing has the potential to offer solutions to produce personalised drug loaded devices, adapted in shape and size to individual patients.

1. Introduction

A large proportion of the population is affected by acne vulgaris (acne), particularly postpubescent teenagers [1, 2]. Acne is a multifactorial chronic inflammatory skin disease commonly found on the face. It originates in the pilosebaceous units and is classified based on the level and severity of the inflammation as open comedones, closed comedones, papules, pustules or nodules. Two of the factors that lead to acne formation are perifollicular hyperkeratinization and follicular obstruction. Androgens, lipids, specific bacteria and cytokines induce hyperkeratinization and hyperproliferation of keratinocytes promoting follicular obstruction and formation of microcomedones [1, 3]. The disorder does not only affect patients physically but also psychologically, leading in some cases to suicide attempts [1, 4].

Most of the topical treatments, generally used for mild to moderate acne, aim to eradicate the pathogenic factors [1, 4]. Salicylic acid is one of the most widely used anti-acne agents; it is a lipophilic β-hydroxyl acid that acts as an anti-inflammatory and exfoliating agent. It penetrates through the skin and detaches corneocytes from each other, weakening the intracellular cement. As a result, the skin cell turnover increases, removing the comedones. Additionally, it improves the elasticity of the stratum corneum and stimulates the production of new corneocytes and collagen [5]. Salicylic acid is found in topical formulations such as creams, gels, cleansers and soap bars with concentrations ranging from 1 to 2% [4]. The commercial treatments containing salicylic acid have high efficacy but they sometimes cause mild and transient side effects (erythema, dryness, intense exfoliation and crusting) which are dependent on dose. The absorption of salicylic acid via topical treatment is enhanced when the formulation comprises a hydrophilic base or is kept occluded.

Three-dimensional printing (3DP) is an additive manufacturing process that allows the fabrication of three-dimensional solid objects of virtually any shape from a 3D model file. The 3D models can be generated by computer aided design (CAD) software or obtained from 3D scanners that capture images and distance information of real objects and then transfer the data to a computer. The implementation of 3D printing technologies has been increasingly growing in many fields. In the pharmaceutical field, 3DP has been used for the production of personalised medicines, oral dosage forms, medical devices, and for tissue engineering [6].

Of the several 3D printing technologies commercially available, fused deposition modelling (FDM) is perhaps the most widely used in pharmaceutics. FDM is simple and cost effective and

has been shown extremely versatile in the development of drug delivery systems [7], especially personalised medicines [8], and medical devices [9, 10]. In FDM an extruded polymer filament is passed through a heated nozzle that softens the polymer and it is then deposited on a build plate, creating one layer of the object to be printed. The build plate then lowers vertically and another layer is deposited. The object is fabricated by repeating these steps in a layer-by-layer manner. The main polymers used in FDM are PLA (polylactic acid or polylactide) and ABS (acrylonitrile butadiene styrene), although an increasing number of polymers is becoming commercially available.

Polycaprolactone (PCL) is a biocompatible polyester with many applications that has been used in wound dressings, tissue engineering and drug delivery, leading to a several PCL drug-delivery devices being approved by the FDA [11-13]. The use of flexible polymers would allow the manufacture of more comfortable devices that are, at the same time, robust to handle. NinjaFlex® (NF) and Flex EcoPLA™ (FPLA) are some of the most widely used flexible filaments. NF is a thermoplastic polyurethane, which is a biomaterial that due to its biocompatibility and mechanical properties is currently used broadly for regeneration, bone replacement and drug/gene delivery [14]. FPLA is a flexible variety of PLA, which is an aliphatic polyester that is degradable in the human body and in the environment, with appropriate mechanical strength and low toxicity [13].

An alternative 3D printing technology that is becoming more affordable is stereolithography (SLA). In this technology, the production is based on the solidification of a liquid resin by photopolymerization. A laser beam causes localized polymerization (solidification) of photocrosslinkable polymers to form a solid layer and the process is repeated in a layer-by-layer manner until the solid 3D object is produced. This technology has been used in the fabrication of oral tablets [15], for tissue engineering [16, 17] and shows higher resolution than the FDM technology [18]. Over the past few years a number of photocrosslinkable polymers have been developed, such as poly(ethylene glycol) diacrylate (PEGDA) [19, 20].

The aim of this work was to evaluate the feasibility of printing anti-acne patches/masks personalised to the anatomy of the patient by 3D scanning and 3D printing. Two different 3D printing technologies - FDM and SLA - were evaluated in terms of manufacture capability, morphological characteristics of the printed object, drug stability while printing and drug release.

2. Materials and Methods

Materials

NF (NinjaFlex® filament, thermoplastic polyurethane, printing temperature 220−230°C, batch no: 3D3071175) and FPLA (Flex EcoPLA™ BLUE 45D filament, flexible polylactic acid, printing temperature 210°C, number: 001) were purchased from iMakr, UK. PCL (Polycaprolactone, 6-caprolactone polymer, $(C_6H_{10}O_2)_n$, MW: 80,000 Daltons, lot no: MKBR4733V), PEGDA (poly(ethylene glycol) diacrylate,, MW: 700 Daltons), PEG (poly(ethylene glycol) 300, MW: 300 Daltons) and diphenyl(2,4,6-trimethylbenzoyl)phosphine oxide were purchased from Sigma Aldrich, UK. Salicylic acid (lot no: 14G020009) was purchased from VWR International, UK. Tetrahydrofuran (THF, HPLC grade) was supplied by Fisher Scientific, UK; dichloromethane (DCM, >99.5% purity) was supplied by VWR International, UK; methanol (≥ 99.9% purity, HPLC grade) was supplied by Sigma Aldrich, UK. The salts for preparing the buffer dissolution media were purchased from VWR International Ltd., Poole, UK.

Methods

2.1 3D scanning

3D scanning of the face of a volunteer was performed with a commercial scanner (Sense™ 3D scanner, 3D Systems Inc., USA) at a distance of 40 cm in accordance with the manufacturer's instructions. The 3D scanner was panned 360° around the head of the subject to capture a 3D image that was exported to Meshmixer (v.10.9.332, Autodesk Inc., USA) to extract the final 3D template for 3DP. A nose-shaped mask (41.2 mm length x 34.5 mm width x 22.7 mm height) adapted to the physical characteristics of an individual was used as 3D model in order to the intricate shape of the design allowed the evaluation of the resolution of the different 3D printing technologies.

2.2 Fused deposition modelling

2.2.1 Preparation of the drug loaded polymers for HME by solvent casting

Before the HME process, polymer (29.4 g) - NF, FPLA or PCL - was dissolved in organic solvent (200 mL) with salicylic acid (0.6 g) using an overhead stirrer. For NF and PCL, THF was used as the solvent while DCM was used for FPLA. The solution obtained after overnight stirring was transferred to Teflon Petri dishes and maintained in a fume cupboard until evaporation of the solvent was accomplished (room temperature, for 2 days). The casted films obtained were stored in an oven (40°C, for 3 days) to completely remove the solvent and, finally, cut into small

pieces to make them suitable for extrusion. The theoretical loading of salicylic acid in the polymer was 2% w/w. Blank filaments were prepared following the same process without addition of the drug.

2.2.2 Hot melt extrusion (HME)

The previously prepared pieces of polymer-salicylic acid were loaded into a single-screw filament extruder (Filabot®, USA) to obtain 1.75 ±0.1 mm diameter polymer filaments for 3D printing. The extruding temperatures were 170°C for NF- salicylic acid, 190°C for FPLA-salicylic acid and 60°C for PCL-salicylic acid. The diameter of the filament was randomly measured with a ProMax Electronic Calliper (Fowler High Precision, USA) at different positions along the filament. Drug loading of the filaments was determined by HPLC analysis (see below).

2.2.3 FDM 3D printing

Devices were fabricated from the drug-loaded filaments using a commercial fused-deposition modelling 3D printer, MakerBot Replicator 2X (MakerBot Inc, USA). The templates used to print the devices obtained by 3D scanning were modified with AutoCAD 2014® (Autodesk Inc., USA) and exported as a stereolithography file (.stl) into the 3D printer software (MakerWare v. 2.2.2, MakerBot Inc., USA). The .stl format encodes only the surface data of the object to be printed and requires the thickness of the surface, the infill and the temperature to be defined in order to print the desired object. The printing parameter settings are shown in **Table 1**.

Table 1

FDM printing settings

Parameters	Polymer	
	FPLA	PCL
Printing temperature (°C)	230	170
Infill (%)	100	100
Number of shell	2	2
Layer height (mm)	0.2	0.1
Speed while extruding (mm/s)	90	50
Speed while travelling (mm/s)	150	50
Raft	No	No
Support	No	No

2.3 Stereolithography (SLA) 3D printing

Two different formulations were printed by SLA 3D Printing: PEGDA/PEG (4:6) and PEGDA/PEG (8:2). To do so, two photopolymer solutions were prepared mixing PEGDA and PEG 300 in different ratios to make a total volume of 40 mL. The photoinitiator, diphenyl(2,4,6-trimethylbenzoyl) phosphine oxide was then added to the mixture solution to a concentration of 1% w/v. Finally, salicylic acid was added into the solution to a concentration of 2% w/w.

Devices were fabricated from the drug-loaded solutions using a commercial SLA 3D printer (Form 1+ Stereolithography 3D printer, Formlabs, UK) equipped with a 405nm laser. The templates used to print the devices were the same as for FDM. They were exported as a stereolithography file (.stl) into the 3D printer software (Preform Software v. 1.9.1, Formlabs, UK). In the settings of the 3D printer, the layer thickness was 0.1mm and the material selection was flexible.

2.4 Characterisation of the filaments and 3D printed objects

2.4.1 Mechanical evaluation of the filaments

An Instron® 5900 Series (Instron, UK) equipped with a 100 N load cell was utilized to carry out tensile tests of standardized filaments (in terms of diameter and length). The equipment was controlled by BlueHill software selecting the default tensile test method. Prior to the test, the system was calibrated for balance length of extension (mm) and load (N).

The filaments were fixed vertically to the clamps of the equipment and stretched gradually during the test until a rupture point or irregular deformation was observed (n=4). The distance between the two clamps was adjusted to 30mm and the diameter and length of tested filament was introduced in the software for the calculation of Young's modulus from the strain-stress curve automatically plotted by BlueHill software. Young's modulus is calculated in the linear region as stress divided by strain.

2.4.2 Thermal analysis

DSC measurements were performed with a Q2000 DSC (TA instruments, Waters, LLC, USA) at a heating rate of 10°C/min. Calibration for cell constant and enthalpy was performed with indium (T_m = 156.6°C, ΔH_f =28.71 J/g) according to the manufacturer's instructions. Nitrogen was used as a purge gas with a flow rate of 50 mL/min for all the experiments. Data were collected with

TA Advantage software for Q series (version 2.8.394), and analysed using TA Instruments Universal Analysis 2000. All melting temperatures are reported as extrapolated onset unless otherwise stated. TA aluminium pans and pin-holed hermetic lids (T_{zero}) were used with an average sample mass of 8-10 mg.

For TGA analysis, samples (average weight: 3-5 mg) were heated at 10°C/min in open aluminium pans with a Discovery TGA (TA instruments, Waters, LLC, USA). Nitrogen was used as a purge gas with a flow rate of 25 mL/min. Data collection and analysis were performed using TA Instruments Trios software and % mass loss and/or onset temperature were calculated.

2.4.3 X-ray powder diffraction (XRPD)

Discs (23.78 mm diameter x 1.00 mm height) made from pure polymers or drug-loaded polymers were printed and analysed. A sample of pure salicylic acid was also analysed. The X-ray powder diffraction patterns were obtained in a Rigaku MiniFlex 600 (Rigaku, USA) using a Cu Kα X-ray source (λ=1.5418Å). The intensity and voltage applied were 15 mA and 40 kV. The angular range of data acquisition was 3–60° 2θ, with a stepwise size of 0.02° at a speed of 5°/min.

2.4.4 Scanning Electron Microscopy (SEM)

The Surface and cross-section images of the filaments and the printed devices were captured with an FEI Quanta 200F Scanning Electron Microscope (FEI, UK). The voltage and working distance were set at 5 V and 50 mm, respectively. Filament samples for SEM imaging were previously coated with gold. Pictures of the 3D printed devices were taken with a Nikon CoolpixS6150 with the macro option of the menu.

2.4.5 Determination of the drug content

For filaments and FDM printed devices, a section of the drug-loaded filament and the 3D printed objects (approx. 0.50 g) was placed in a volumetric flask (25mL) with the appropriate organic solvent (THF was used for NF and PCL while DCM was used for FPLA) under magnetic stirring until complete dissolution. Aliquots (10 mL) were transferred to a volumetric flask with methanol (40 mL) to precipitate the polymer. The solution was then filtered through a 0.22 μm filter (Millipore Ltd., Ireland) and the concentration of drug in the filtrate was determined by HPLC.

For SLA printed devices, a section of the drug-loaded 3D printed mask (approx. 0.50 g) was milled with mortar and pestles and placed into a volumetric flask with methanol (25mL) under magnetic stirring until complete dissolution of the drug. The solution was then filtered through a 0.22 µm filter (Millipore Ltd., Ireland) and the concentration of drug in the filtrate was determined by HPLC (see below).

The HPLC (Hewlett Packard 1050 Series HPLC system, Agilent Technologies, UK) assay entailed injecting samples (20.0 µL) into a mobile phase consisting of methanol (70%) and 0.1% trifluoroacetic acid (TFA) in water (30%), through a reverse phase column (Ascentis® C18, 5 µm particle size, 4.6 × 150 mm) connected with a pre-column all maintained at 25°C. The mobile phase was pumped at a flow rate of 1.0 mL/min and the eluent was screened at the wavelength of 234 nm.

2.4.6 Diffusion studies

Drug diffusion experiments from circular-shaped 3D printed devices (16 mm diameter and 1 mm thickness) were conducted in vertical glass Franz cells with an effective diffusion area of 98.5 ± 4.8 mm^2 and a receptor volume of 4.6 mL (n=3).

The 3D printed patches were mounted between the donor and receptor compartments, separated from the receptor by a cellulose nitrate membrane (pore size 0.45µm, cat no. 7184-002, Whatman, UK) previously soaked in receptor fluid for at least 12 hours before starting the test was started. The receptor compartment of the diffusion cell was filled with phosphate-buffered saline (Dulbecco A, Thermo Scientific, UK) at pH 7.3

The whole assembly was incubated at 32°C in a water bath in order to mimic the skin temperature and the solution in the receptor compartment was constantly stirred at 400 rpm using a magnetic stirrer. Donor (with no solution) and receptor compartments were occluded with Parafilm to prevent evaporation.

At different intervals, 200 µL aliquots were withdrawn from each cell and replaced with an equal amount of phosphate-buffered saline. The drug concentration was then determined by HPLC. The cumulative percentages of drug permeated per square centimetre from the 3D printed patches were plotted against time.

3. Results and discussion

3D scanning

The 3D scanning process performed with the commercial Sense™ 3D scanner showed good resolution (according to the manufacturer, the point-to-point spacing is around 0.65mm), capturing the object with the real size without the need of calibration (**Fig. 1A**). The quality of the scanning process is dependent on the experience of the operator and the light conditions, but the system is easy to operate with basic training. The scanning process can be performed without contact in a few seconds, so it could be useful for people who have difficulties remaining still and as a fast/routine technique.

A section of the model obtained from the 3D scan (the nose of the volunteer) was selected as a model for 3D printing due to the prevalence of acne localized in that region and the challenge of printing intricate shapes (**Fig. 1B**). The use of CAD software (Meshmixer) easily allowed the selection of specific parts to be printed. In this case, the internal part of the nose design was designed hollow, to fit perfectly on the nose of the individual.

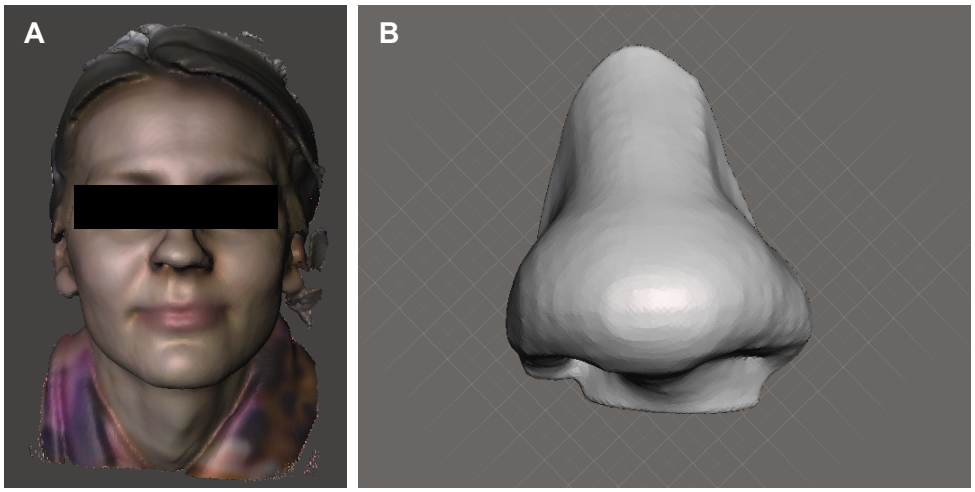

Fig. 1. A) Volunteer scanning image and B) 3D model nose used for 3DP.

Fused Deposition Modelling (FDM) 3DP

It was possible to produce drug-loaded filaments by HME incorporating salicylic acid into the polymers; however, for the commercial filaments the characteristic of the filaments changed considerably by inclusion of the drug and were significantly different from the commercial filament in terms of size, physical appearance and mechanical behaviour.

The NF-salicylic acid filament obtained from HME became red-brown with a rough surface and brittle after being extruded. It was so brittle that it was not possible to hold it in the Instron equipment to determine Young's modulus. The SEM images show that the NF-salicylic acid filament had an irregular surface and inconsistent morphology (cross section not circular) compared with commercial NF (**Fig. 2A and 2B**). According to the manufacturer's material safety data sheet (MSDS), NF is made of polyurethanes and its properties are highly affected by solvents and acids [21]. It has also been reported that salicylic acid is incompatible with polyurethanes, affecting physical properties of the polymer, such as tensile strength, hardness and elongation [22]. Consequently, the NF-salicylic acid filament was significantly different from the NF filament in terms of flexibility and colour, which made the filament not suitable for 3D printing.

The FPLA-salicylic acid filament (1.67 ±0.16 mm diameter) showed a surface as smooth as the commercial FPLA filament (1.75 ±0.02 mm diameter) (**Fig. 2C and 2D**). The colour of the FPLA-salicylic acid filament was slightly darker compared with the commercial FPLA, however the flexibility of the filaments was comparable. Young's modulus of FPLA-salicylic acid and commercial FPLA filament was 93.53 ± 4.34 MPa and 93.17 ± 3.72 MPa respectively.

The PCL-salicylic acid filament was white, smooth and with good morphology (uniform diameter, 1.65 ±0.11 mm), comparable to that of the PCL filament obtained from PCL pellets without drug by HME (**Fig. 2E and F**). Young's modulus of PCL-salicylic acid (286.43 ± 25.23 MPa) and not drug-loaded PCL filament (280.39 ±25.92 MPa) are similar, but stiffer than FPLA filaments (Young's modulus ~93 MPa).

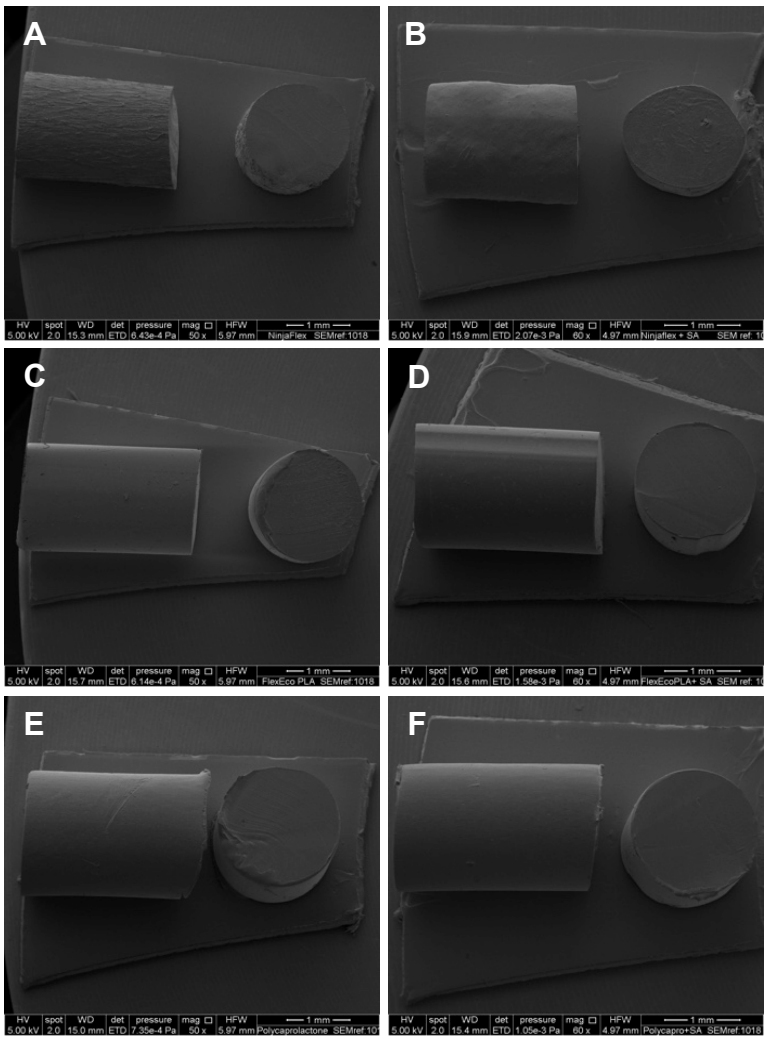

Fig. 2. SEM images of A) commercial NF filament, B) the NF-salicylic acid filament, C) commercial FPLA filament, D) FPLA-salicylic acid filament, E) plain PCL filament prepared from PCL pellets and F) PCL-salicylic acid filament.

The drug loading of the FPLA-salicylic acid filament was 0.63 ± 0.10% w/w. It is evident that the extrusion process causes degradation of salicylic acid (theoretical drug loading 2% w/w), which was a result of the high extruding temperature (190°C). The drug loading in the PCL-salicylic acid filament was 1.34 ± 0.01% w/w. The amount of salicylic acid in the PCL filament is higher than that in the FPLA filament because the extrusion temperature is much lower (60°C), so the salicylic acid remains more stable during extrusion, but this still represents a significant degree of degradation.

TGA data show also signs of drug degradation (**Fig. 3**). The amount of salicylic acid at different temperatures compared with the starting amount in terms of percentage implies the degradation temperature range of the tested substance. The percentage of weight of salicylic acid is greatly reduced at the temperature above 140°C and salicylic acid completely degraded at the temperature about 200°C (**Fig. 3**).

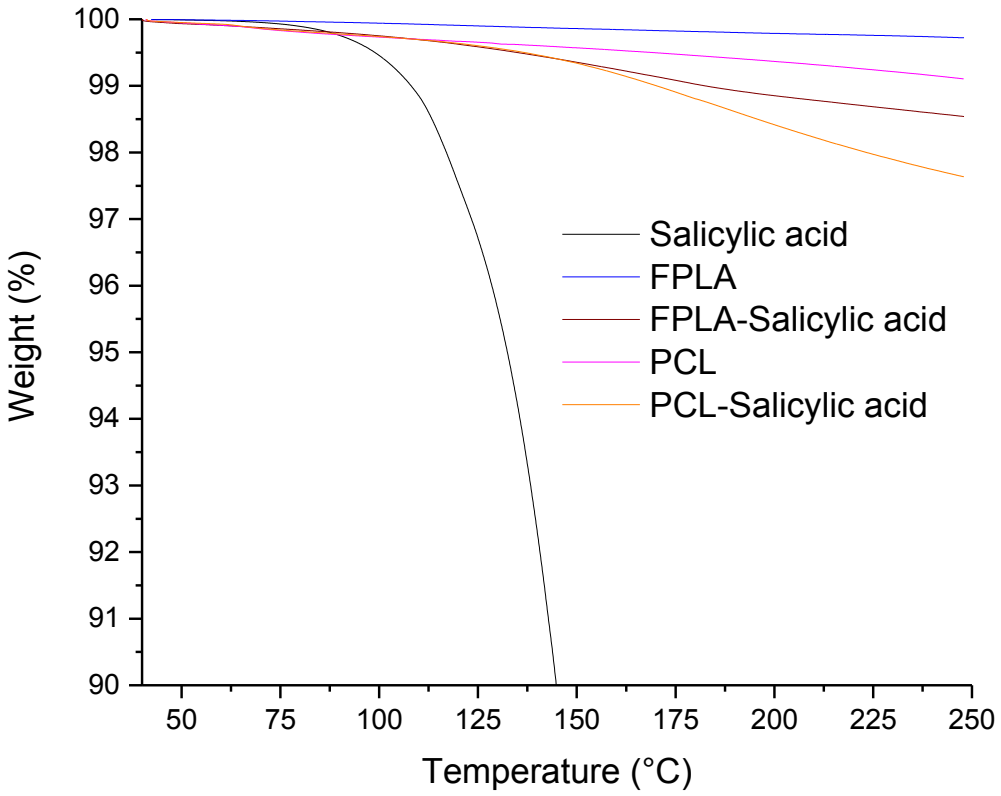

Fig. 2. TGA results for Salicylic acid (SA), the extruded filaments (blank) and the drug loaded filaments.

The weight loss percentage for the FPLA-salicylic acid filament was higher than non-drug loaded filament by approximately 1.5%, which corresponded to salicylic acid degradation and reduced heat stability of the polymer due to hydrolysis. It was assumed that salicylic acid hydrolysed ester bonds of the polymer, resulting in decreased strength and heat stability of the polymer [23]. However, the stability of the FPLA-salicylic acid filament was acceptable at the printing temperature since the weight loss percentage was not significant.

The mass of PCL-salicylic acid filament decreased more than the non-drug loaded PCL filaments at temperatures above 200°C. This may be because the incorporation of drug into PCL affects the properties of polymer, reducing heat stability.

For the 3D printing process, sections of filaments with the diameter closer to the optimum for the FDM printer (1.75mm) were selected. The FPLA-salicylic acid filament was successfully printed as a flat circular patch. The quality of printing was considered good, as the shape was well defined and there were no printing inconsistencies. Pure PCL and the PCL-salicylic acid filaments were also successfully 3D printed as circular patches. As mentioned previously, the NF-salicylic acid filament was not printable due to the lack of flexibility (and so NF-salicylic acid filament was not further evaluated in this study).

The evaluation of the drug loading from 3D printed devices showed lower values to those of the drug–loaded filaments used for printing, indicative of degradation during the 3DP process. The mean amount of salicylic acid content in the FPLA-salicylic acid printed circle was 0.35 ± 0.01% w/w. This shows that the percentage of salicylic acid in the 3D printed device decreases compared with the initial percentage of drug in the filament because of the printing process, which was performed at 230°C. The mean amount of salicylic acid content in the PCL-salicylic acid printed patch was 1.21 ± 0.02% w/w, which indicates that some salicylic acid in the filament decomposed while 3D printing at 170°C. The decomposition of the drug while printing, due to the heat involved process, has been noted previously [24].

The XRD data reveals that FPLA is semi-crystalline because crystalline peaks and an amorphous halo are noticeable (**Fig. 4**). However, the XRD data of the FPLA-salicylic acid could not confirm the physical form of salicylic acid in the formulation. There are not peaks similar to those in the XRD pattern of pure salicylic acid powder, which indicates that the drug is either dissolved in the polymers or it is not detected due to the low drug loading percentage.

PCL is also in a semi-crystalline form as the XRD pattern consists of both crystalline peaks and an amorphous halo (**Fig. 4**). No evidence for salicylic acid as a crystalline phase was seen in the PCL-salicylic acid XRD data.

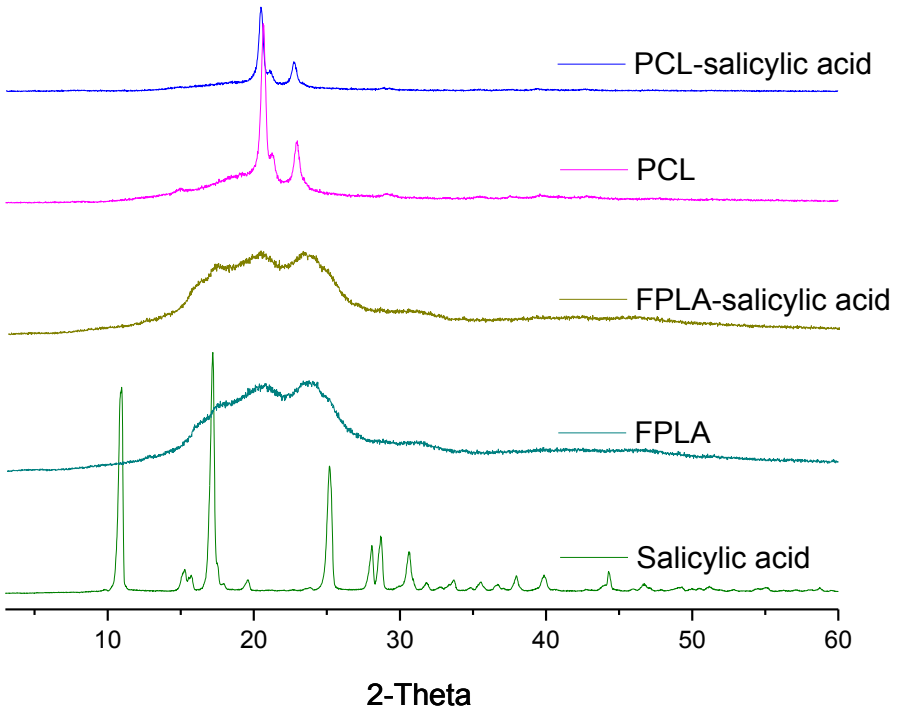

387

388 **Fig. 4.** X-ray powder diffraction patterns for salicylic acid and various FDM printed discs

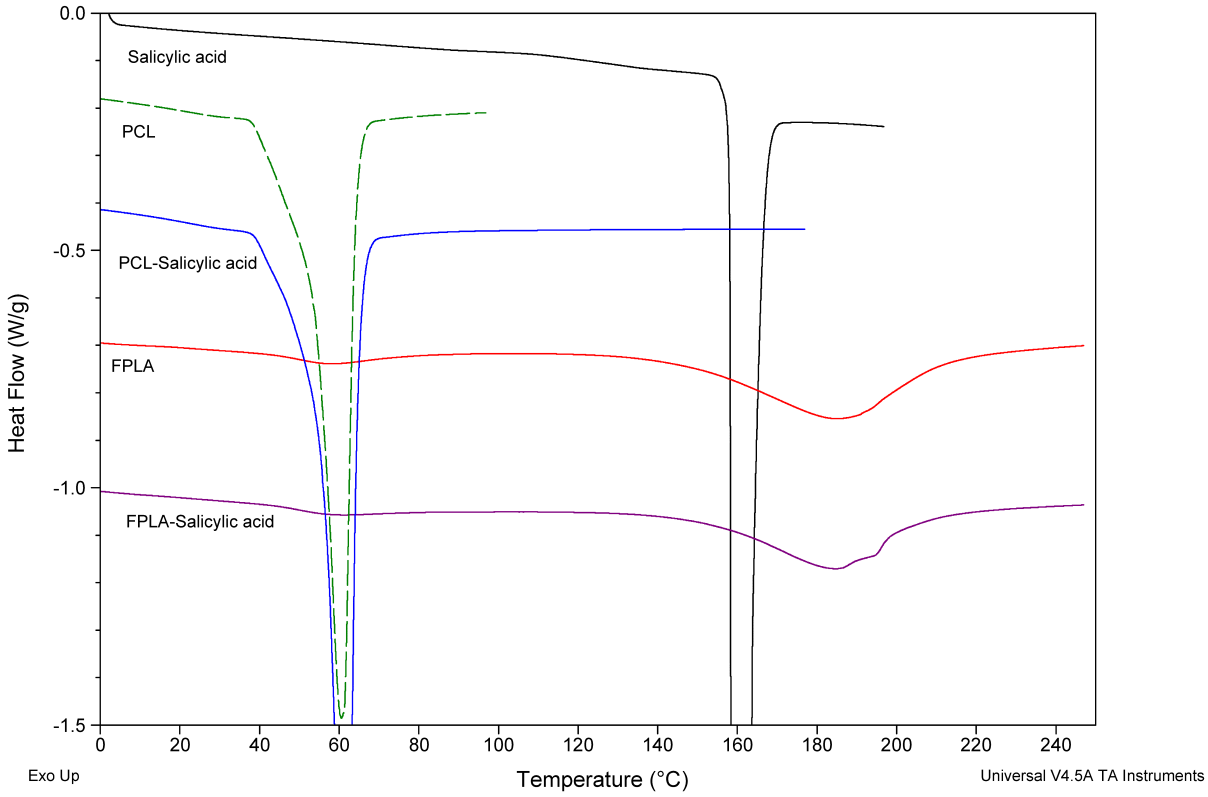

389

Fig. 5. DSC thermal traces for salicylic acid and various FDM printed discs

The DSC thermograms for salicylic acid show a sharp endothermic peak (melting point, T_m) at 160°C (**Fig. 5**). This implies that salicylic acid powder was in the crystalline form. The comparable DSC profiles of FPLA and FPLA-salicylic acid discs are shown in **Fig. 5**. A salicylic acid melt is not seen in the FPLA-salicylic acid disc. Although the T_m of FPLA patch (187°C) is slightly higher compared with the two endothermic peaks at 183°C and 202°C that became a combined peak with T_m of 185°C of FPLA-SA, the overall properties of FPLA are not significantly affected by the presence of SA. For the PCL, PCL-salicylic acid disc does not show the melting peak of the SA, and PCL printed disk shows also similar T_m (60°C) to the T_m of the PCL-salicylic acid disc (61°C).

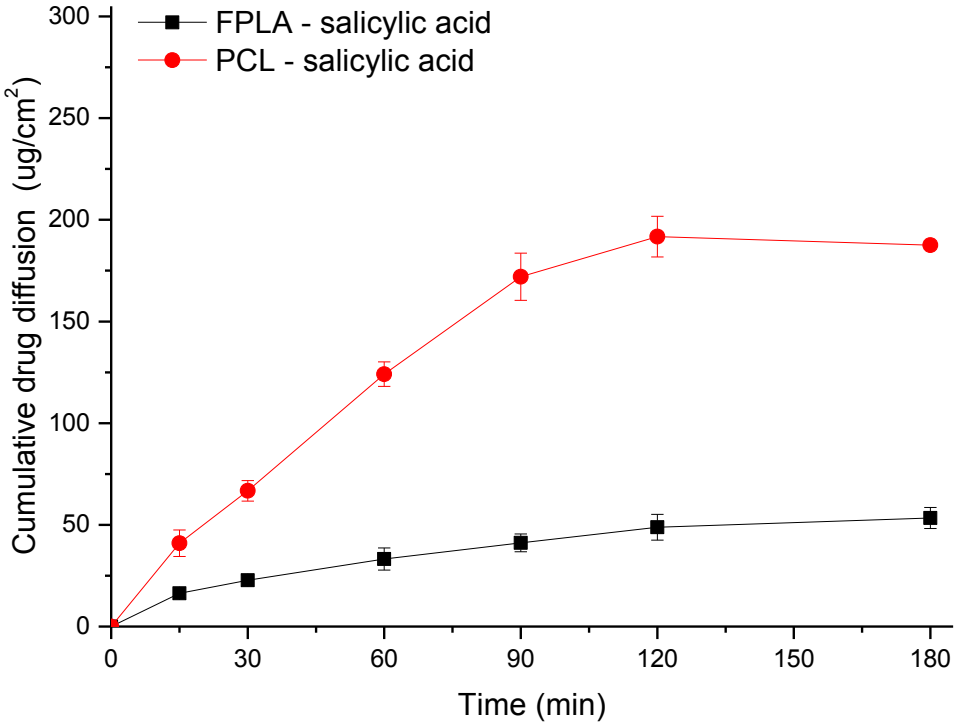

Fig. 6. Cumulative amounts of salicylic acid permeated from the FDM 3D printed devices.

Drug permeation from the patches occured slowly (**Fig. 6**), as expected for a topical drug delivery device (even though the synthetic membrane used is considered as a high flux material [25]).

The PCL-salicylic acid printed sample showed a higher rate of drug diffusion than the FPLA-salicylic acid. The release profiles show that the cumulative percentage of drug diffused from the printed FPLA-salicylic acid patch was 16 and 22μg/cm^2 at 15 and 60 min, respectively. For the 3D printed PCL-salicylic acid sample the values were higher; 40 and 66 μg/cm^2 at 15 and 60 min, respectively. In use, such a mask could be worn on numerous occasions since the maximum diffusion reached only 191 μg/cm^2.

Regarding the printing of intricate devices/masks, the FPLA-salicylic acid printed nose was successfully obtained with the same printing settings as for the FPLA-salicylic acid circular patch. The printed nose was flexible and the shape was clearly defined, although some parts of the nose had small gaps between layers due to the inconsistency of the printing process.

The nose mask could not be printed using the PCL-salicylic acid filament. At the printing temperature used to print the patch from the PCL-salicylic acid filament (170°C) the layer cooled down slowly and failed to solidify to form stable layers in the curved regions of the nose. Lower temperatures resulted in blockage of the nozzle of the printer. The use of lower printing speed or extra fans to cool it down faster may allow the fabrication of structures more complex than a flat patch.

SLA printing

It was possible to fabricate patches incorporating drugs by SLA printing. The composition of the formulations included the photocrosslinkable polymer PEGDA and PEG that was added as a filler. PEG chains are interspersed with the PEGDA chains, which reduces the degree of crosslinking between PEGDA chains. The PEGDA/PEG-salicylic acid patches were smooth and slightly flexible; those with higher amounts of PEG: PEGDA/PEG (4:6)-salicylic acid were most flexible.

The salicylic acid content in the devices obtained by SLA was 1.95 ± 0.04% w/w for the PEGDA/PEG (4:6)-salicylic acid and 1.96 ± 0.03% w/w for the PEGDA/PEG (8:2)-salicylic acid, both higher than that in the devices prepared by FDM 3DP and very close to the expected value. Since fabrication of the mask by SLA printing is not based on heat, unlike FDM 3DP,, salicylic acid is not thermally degraded and remains in the mask at a higher concentration.

XRPD results suggest that salicylic acid is present in the amorphous phase within the patches as no peaks appeared in the patterns of these formulations (**Fig. 7**). The drug is completely dissolved in the photopolymer solution while printing and according to these results there is no crystallization of the drug during the photopolymerization process. DSC data confirm that extent since no drug endotherm peak is observed (Fig. 8)

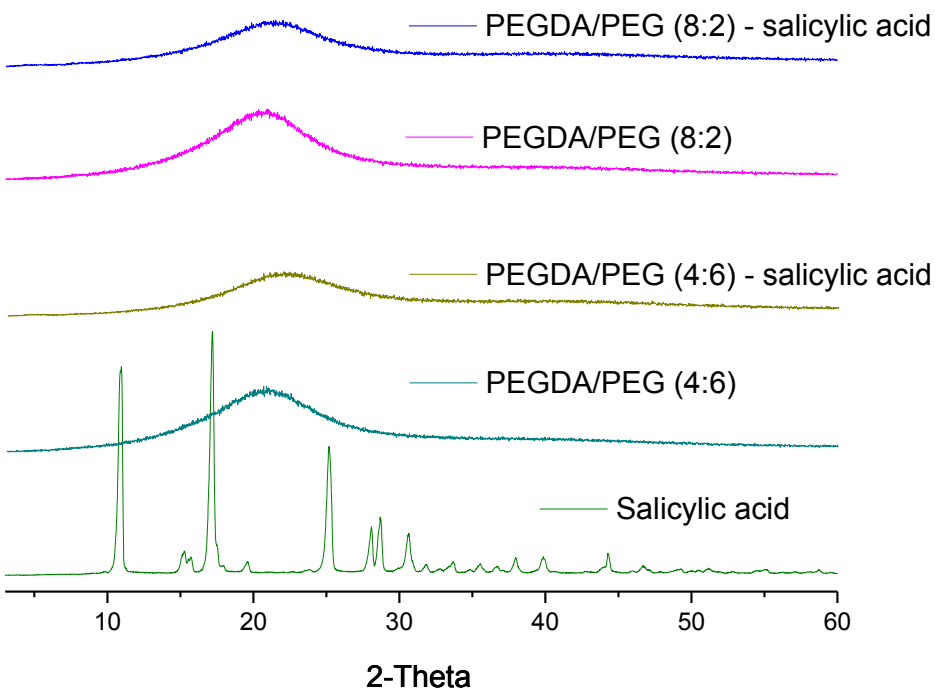

Fig. 7. X-ray powder diffraction patterns for salicylic acid and various SLA 3DP polymer discs.

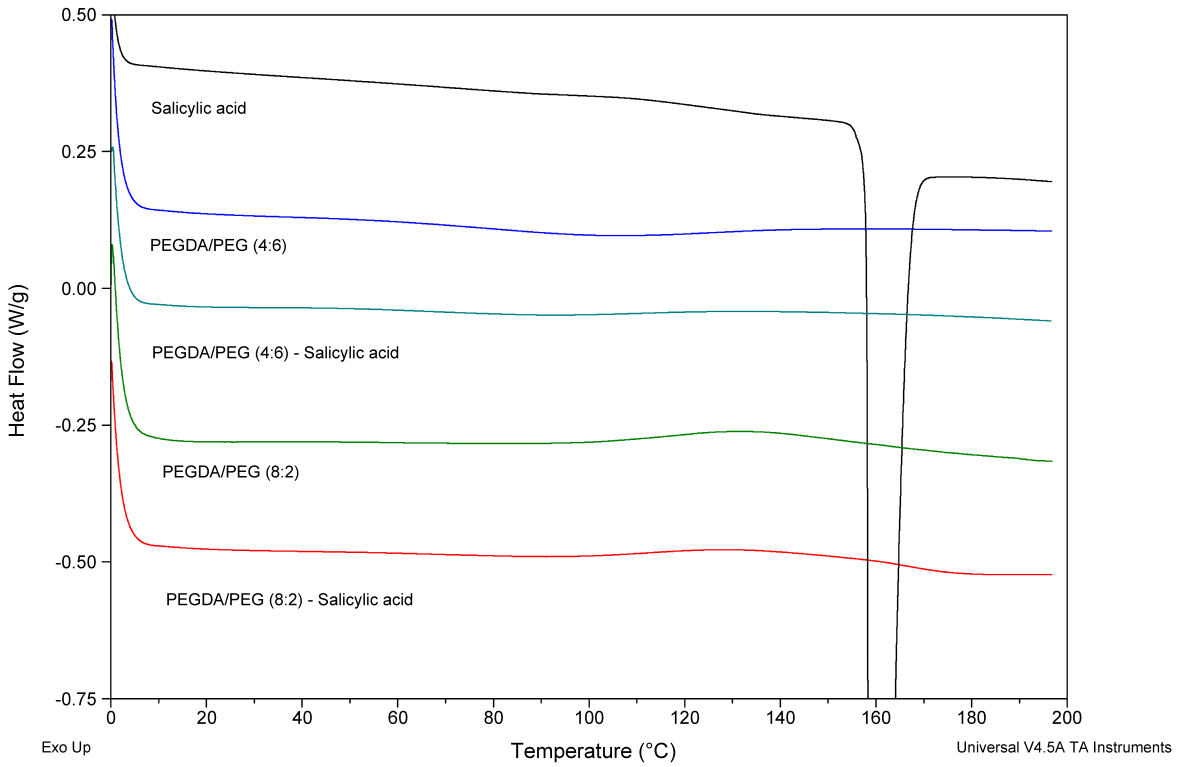

Fig. 8. DSC thermal traces for salicylic acid and various SLA 3DP polymer discs .

Drug diffusion from the two 3D printed devices manufactured by SLA was higher than that obtained from devices printed by FDM 3DP after 3h (**Fig. 9**). The diffusion profiles show that the cumulative percentage of drug diffused from the printed PEGDA/PEG patch with the higher amount of PEG is similar (25 and 48 μg/cm^2 at 15min and 60 min, respectively) to that with lower amount of PEG (30 and 45 μg/cm^2 at 15min and 60min) during the first 2 h. After this time diffusion is faster from patches with higher amount of PEG. A possible explanation is that the PEG gets dissolved in the dissolution media, forming pores that let the media have improved access to more internal regions of the devices easier and faster than in less porous devices. The effect of the PEGDA/PEG ratio was previously described for oral tablets prepared by SLA printing [15].

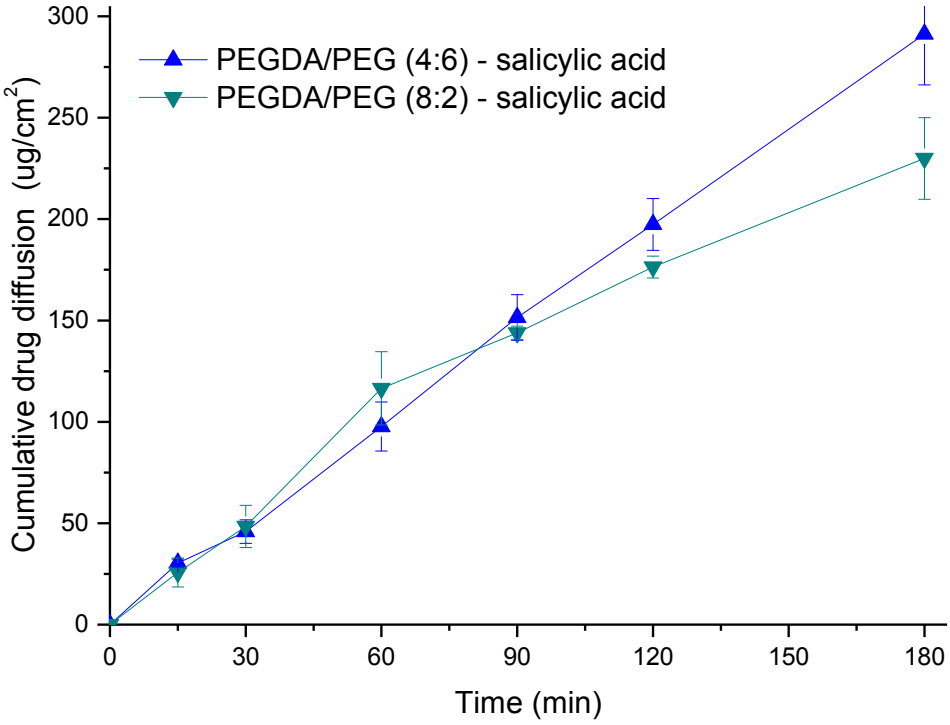

Fig. 9. Cumulative amounts of salicylic acid permeated from the devices 3D printed by SLA.

For the fabrication of the nose-shaped device containing salicylic acid, SLA 3DP provided higher resolution than the FDM approach (**Fig. 10**). The mask is as flexible as the mask obtained from FDM 3DP with the flexible polymer FPLA-salicylic acid.

Fig. 10. Nose-shaped device fabricated by SLA 3D printing PEGDA/PEG (4:6)-salicylic acid.

Conclusions

3D printing technologies show potential in the development of personalized anti-acne drug loaded masks/patches. In FDM 3DP, the use of HME produced filaments of FPLA-salicylic acid and PCL-salicylic acid with uniform diameter and suitable for 3D printing, whereas the NF-salicylic acid filament was too brittle for 3D printing. Drug loading was higher in 3D printed objects obtained with PCL-salicylic acid filaments than with FPLA-salicylic acid filaments due to the greater degradation of the drug at higher temperatures (extrusion and 3D printing). However, the resolution and printing characteristics of the objects were better with FPLA-salicylic acid, it was not possible to print nose-shaped mask with the PCL-salicylic acid filament.

Drug diffusion tests conducted in Franz cells revealed that FPLA-salicylic acid and PCL-salicylic acid printed samples diffused only 53 and 187 $\mu g/cm^2$ respectively within 3 h.

SLA printing involves a one-step process that leads to 3D printed devices with higher resolution than the obtained with the FPLA-salicylic acid filaments and with higher drug loading than the PCL-salicylic acid filament (1.9% w/w), with no drug degradation. The results of drug diffusion tests conducted under the same conditions revealed that the total drug diffused is also faster than with the FDM approaches, 291 $\mu g/cm^2$ within 3 hour for PEGDA/PED (4:6)-salicylic acid and 229 $\mu g/cm^2$ for the PEGDA/PED (8:2)-salicylic acid.

Therefore it can be concluded that SLA printing is a more convenient 3D printing technology to manufacture anti-acne devices with salicylic acid. The 3D printed masks may be considered as promising formulations that can be developed further to provide higher efficacy in acne treatment. The dose of drug may be adjusted (reduced) to personalize the device by incorporating a specific dose of drug into the polymer that will then be printed as a patch for each patient, maybe ameliorating the dose-dependent side effects of the treatment. In other pathologies, the combination of 3D scanning and 3D printing, have the potential to offer solutions to produce personalised drug loaded devices, adapted in shape and size to individual patients.

References

[1] S. Das, R.V. Reynolds, Recent Advances in Acne Pathogenesis: Implications for Therapy, Am. J. Clin. Dermatol., 15 (2014) 479-488.

[2] J.K.L. Tan, K. Bhate, A global perspective on the epidemiology of acne, Br. J. Derm., 172 Suppl 1 (2015) 3-12.

[3] S. Knutsen-Larson, A.L. Dawson, C.A. Dunnick, R.P. Dellavalle, Acne vulgaris: pathogenesis, treatment, and needs assessment, Dermatol. Clin., 30 (2012) 99-106, viii-ix.

[4] R. Nguyen, J. Su, Treatment of acne vulgaris, Paediatr. Child Health, 21 (2011) 119-125.

[5] S. Ramanathan, A.A. Hebert, Management of acne vulgaris, J. Pediatr. Health Care, 25 (2011) 332-337.

[6] C.L. Ventola, Medical Applications for 3D Printing: Current and Projected Uses, P&T, 39 (2014) 704-711.

[7] A. Goyanes, J. Wang, A. Buanz, R. Martinez-Pacheco, R. Telford, S. Gaisford, A.W. Basit, 3D Printing of Medicines: Engineering Novel Oral Devices with Unique Design and Drug Release Characteristics, Mol. Pharm., 12 (2015) 4077-4084.

[8] A. Goyanes, A.B. Buanz, A.W. Basit, S. Gaisford, Fused-filament 3D printing (3DP) for fabrication of tablets, Int. J. Pharm., 476 (2014) 88-92.

[9] B.C. Gross, J.L. Erkal, S.Y. Lockwood, C. Chen, D.M. Spence, Evaluation of 3D printing and its potential impact on biotechnology and the chemical sciences, Anal. Chem., 86 (2014) 3240-3253.

[10] J.J. Water, A. Bohr, J. Boetker, J. Aho, N. Sandler, H.M. Nielsen, J. Rantanen, Three-Dimensional Printing of Drug-Eluting Implants: Preparation of an Antimicrobial Polylactide Feedstock Material, J. Pharm. Sci., 104 (2015) 1099-1107.

[11] C.L. Salgado, E. Sanchez, J. Mano, A. Moraes, Characterization of chitosan and polycaprolactone membranes designed for wound repair application, J. Mater. Sci., 47 (2012) 659-667.

[12] B.D. Ulery, L.S. Nair, C.T. Laurencin, Biomedical applications of biodegradable polymers, J. Polym. Sci. Part B Polym. Phys., 49 (2011) 832-864.

[13] T. Patrício, M. Domingos, A. Gloria, P. Bártolo, Characterisation of PCL and PCL/PLA scaffolds for tissue engineering, Procedia CIRP, 5 (2013) 110-114.

[14] A.L. Tyson, S.T. Hilton, L.C. Andreae, Rapid, simple and inexpensive production of custom 3D printed equipment for large-volume fluorescence microscopy, Int. J. Pharm., 494 (2015) 651-656.

[15] J. Wang, A. Goyanes, S. Gaisford, A.W. Basit, Stereolithographic (SLA) 3D printing of oral modified-release dosage forms, Int. J. Pharm., 503 (2016) 207-212.

[16] K. Arcaute, B.K. Mann, R.B. Wicker, Stereolithography of three-dimensional bioactive poly(ethylene glycol) constructs with encapsulated cells, Ann. Biomed. Eng., 34 (2006) 1429-1441.

[17] K. Arcaute, B. Mann, R. Wicker, Stereolithography of spatially controlled multi-material bioactive poly(ethylene glycol) scaffolds, Acta Biomater., 6 (2010) 1047-1054.

[18] F.P.W. Melchels, J. Feijen, D.W. Grijpma, A review on stereolithography and its applications in biomedical engineering, Biomaterials., 31 (2010) 6121-6130.

[19] V. Chan, P. Zorlutuna, J.H. Jeong, H. Kong, R. Bashir, Three-dimensional photopatterning of hydrogels using stereolithography for long-term cell encapsulation, Lab Chip., 10 (2010) 2062-2070.

[20] M. Vehse, S. Petersen, K. Sternberg, K.-P. Schmitz, H. Seitz, Drug Delivery From Poly(ethylene glycol) Diacrylate Scaffolds Produced by DLC Based Micro-Stereolithography, Macromol. Symp., 346 (2014) 43-47.

[21] Fenner_Drives, Support technical specifications, http://www.ninjaflex3d.com/support/using-ninjaflex/technical-specifications/, last accessed 04-2016.

[22] PPE_Ltd, A technical guide to Elastomer Compounds and Chemical Compatibility, http://www.prepol.com/Ppe-Uploads/Elastomer_guide_chemical_compatibility.pdf, last accessed 04-2016.

[23] L. Xu, K. Crawford, C.B. Gorman, Effects of Temperature and pH on the Degradation of Poly(lactic acid) Brushes, Macromolecules, 44 (2011) 4777-4782.

[24] A. Goyanes, A.B. Buanz, G.B. Hatton, S. Gaisford, A.W. Basit, 3D printing of modified-release aminosalicylate (4-ASA and 5-ASA) tablets, Eur. J. Pharm. Biopharm., 89 (2015) 157-162.

[25] S.-F. Ng, J. Rouse, D. Sanderson, G. Eccleston, A Comparative Study of Transmembrane Diffusion and Permeation of Ibuprofen across Synthetic Membranes Using Franz Diffusion Cells, Pharmaceutics, 2 (2010) 209-223.